Tellus SERIES B CHEMICAL AND PHYSICAL METEOROLOGY
PUBLISHED BY THE INTERNATIONAL METEOROLOGICAL INSTITUTE IN STOCKHOLM

Tellus (2010), 62B, 259–279
Printed in Singapore. All rights reserved

TELLUS

The role of sea-salt emissions in controlling the marine Aitken and accumulation mode aerosol: a model study

By E. MONICA MÅRTENSSON[1]*, PETER TUNVED[1], HANNELE KORHONEN[2,3] and E. DOUGLAS NILSSON[1], [1]*Department of Applied Environmental Science, Stockholm University, SE-106 91 Stockholm, Sweden;* [2]*Finnish Meteorological Institute, Kuopio Unit, POB 1627, 702 11 Kuopio, Finland;* [3]*Department of Physics and Mathematics, University of Eastern Finland, POB 1627, 702 11 Kuopio, Finland*

(Manuscript received 18 December 2009; in final form 14 June 2010)

ABSTRACT

The remote marine aerosol and the cloud droplet number concentration (CDNC) are examined with an aerosol microphysics box model in an attempt to better understand the processes involved in the formation and transformation of the marine aerosol. Emission of submicrometre sea-salt and dimethylsulfide (DMS) have been included together with aerosol dynamics, gas and liquid phase chemistry and cloud processing representative for the marine boundary layer atmosphere. Our simulations are able to reproduce a bimodal submicrometre size distribution with realistic number concentrations even when new particle formation by nucleation is neglected. This indicates that ultrafine primary sea-salt flux is an important source of Aitken mode particles and CDNC. However, sulphate still constitutes 20–80% of the Aitken and accumulation mode masses. The temperature dependence of the sea-salt source function leads to a 23% decrease in total number concentration when the temperature increases from 12 to 20 °C. The influence of DMS emission on the aerosol and CDNC is minimal but the size distribution and mass concentration of sulphate is changed, mostly due to in-cloud processes. The wind speed is the dominant factor determining the CDNC, although entrainment of aerosols from free troposphere can have a substantial effect.

1. Introduction

About 71% of the Earth's surface is covered by water, helping to explain why sea spray is the largest aerosol source globally in terms of mass, possibly in competition with dust emissions in the Northern Hemisphere (IPCC, 2001). Instead of warming the atmosphere, like the greenhouse gases, marine aerosols cool the atmosphere: directly by scattering the incoming solar radiation and indirectly via clouds where they act as cloud condensation nuclei (CCN). The influence of marine aerosol extends also to continental regions, for example the Amazonian basin (Andreae et al., 1990; Talbot et al., 1990). The chemical composition and the size distribution of the marine aerosol is complex, the primary aerosols generated by breaking waves and bubble bursting varies depending on the composition of the sea water, e.g. different concentrations of dissolved and particular organic carbon). Microphysical processes and chemical reactions in the atmosphere and clouds transform the aerosol, e.g. sulphate that is internally mixed into the particles can originate from natural sources in the sea water and continental and oceanic anthropogenic sources. Over the oceans the marine aerosol can be mixed with a number of different aerosols originating from natural and anthropogenic continental sources, e.g. with Saharan dust or sulphate and soot from biomass burning and combustion of fossil fuels. However, in remote areas the aerosol burden and composition is primarily dictated by oceanic sources.

Numerous studies are available on marine aerosol mass concentrations (e.g. Andreae et al., 1999; Quinn and Coffman, 1999; Cavalli et al., 2004). Furthermore, most marine aerosol size distribution measurements have been obtained during short-term campaigns or cruises (e.g. Covert et al., 1998; Russell and Heintzenberg, 2000; Bates et al., 2002; Huebert et al., 2003). However, Heintzenberg et al. (2004) have evaluated the submicrometre size distributions from four campaigns. Log-normal fits to data resulted in four-modal approximations of the marine size distribution both for the individual experiments and as an average size distribution for the four experiments. Furthermore, the variability of the submicrometre concentration was parametrized which quantified the probability of finding different number concentrations around the median concentrations from these measurements. Details of the chemical composition of the marine aerosol submicrometre particles, especially the ultrafine particles (with diameter less than 0.1 μm) remain unknown despite the fact that several measurement studies have

*Corresponding author.
e-mail: monica@itm.su.se
DOI: 10.1111/j.1600-0889.2010.00465.x

shown significant concentrations of marine particles in the ultrafine size range (e.g. Hoppel et al., 1990; O'Dowd and Smith, 1993; Murphy et al., 1998; Bates et al., 2000; Nilsson et al., 2001; Clarke et al., 2006). One of the best-known and most widely used data sets was collected by O'Dowd et al. (1997), who parametrized sea-salt emissions in the form of three log-normal number size distributions with amplitudes depending on the wind speed. Unfortunately, this parametrization only covers the size range above 100 nm in particle diameter.

Studies of aerosol number fluxes over the oceans are more scarce, although in situ measurements of the marine aerosol number flux have been reported by, e.g. Nilsson et al. (2001), Geever et al. (2005), Nilsson et al. (2007) and Norris et al. (2008). Of these, however, only Nilsson et al. (2007) provides detailed, size-segregated information about the aerosol source function. Mårtensson et al. (2003) and Clarke et al. (2006), have presented parametrizations that cover fully two decades of the submicrometre (down to ~10 nm) production of primary marine aerosols, Mårtensson et al. (2003) showed in a set of laboratory experiments that at least some of these ultrafine particles could have a sea spray origin. This study successfully simulated bubble bursting and thereby production of a sea-salt aerosol. Based on their results, the authors derived a new sea-salt emission parametrization extending the size range down to dry particle diameter, (D_p), of 20 nm. This parametrization includes a function of the whitecap coverage [and hence the wind speed, from Monahan and O'Muircheartaigh (1980)] and a new function for the marine aerosol emission per white cap area, dependent on particle size and water temperature. The parametrization was shown by the authors to be consistent in magnitude with the first direct in situ measurements of the total ($D_p > 10$ nm) aerosol emissions reported in Nilsson et al. (2001). This parametrization has recently been validated in the 0.1–1.1 μm D_p range for temperate water (12 °C) by direct emission measurements using the eddy covariance technique on the Irish west coast (Nilsson et al., 2007). Although not by direct emission measurements, Clarke et al. (2006) estimate emissions from concentration gradients confirming the Mårtensson et al. (2003) results for tropical conditions (25 °C).

The dependence of the emitted size distribution on sea surface water temperature is one of the most interesting features of these new results. Both the laboratory (Mårtensson et al., 2003) and in situ measurements (Nilsson et al., 2007) show that total ($D_p > 20$ nm D_p and $D_p > 10$ nm D_p, respectively) aerosol number emission will decrease with increasing water temperature. However, for particles with $D_p > 100$ nm, the trend is opposite (the number emissions increase with increasing temperature). Since the potential for particles to act as cloud droplets is dependent on particle size, water temperature may be an important factor determining the number of particles activated as cloud droplets originating from sea spray. This effect could in principle be either positive or negative depending on the ambient conditions. A further complication to the picture is that the sea water temperature has also a potential to influence the marine aerosol concentration though its effects on biological activity, sea water layering and upwelling and thus on dimethylsulfide (DMS) emissions from the oceans (Charlson et al., 1987). It remains therefore unclear how the projected changes in sea water temperature as a result of climate change will contribute to the climate feedbacks over the oceans.

Most of the previous model studies on aerosol and CCN formation in the marine boundary layer have used sea-salt particle fluxes without ultrafine contribution (e.g. Capaldo et al., 1999; Yoon and Brimblecombe, 2002; Spracklen et al., 2007). The source of the ultrafine particles has instead been assumed to be nucleation and entrainment of a sulphate aerosol originating from DMS. On the other hand, the modelling studies of Pierce and Adams (2006) and Korhonen et al. (2008) did include ultrafine sea-salt emissions. In their global general circulation model (GCM) study Pierce and Adams (2006) evaluated the importance of the emission of sea-salt aerosols for the formation of CCN. Especially in remote marine areas, where the contribution of anthropogenic SO_2 is low, the emissions of ultrafine ($D_p <$ 100 nm) and accumulation mode sea-salt particles was shown to have a large impact on the CCN concentration. The same study found that the modelled CCN concentration depends strongly on the sea spray source function used. Korhonen et al. (2008) studied sources of marine CCN over the southern hemisphere oceans and found sea spray the dominant source all year round in regions of high surface wind speeds (45–60°S) and in winter over all oceanic regions south of 30°S. On the other hand, they concluded that DMS emissions (via nucleation in the free troposphere, FT) may be responsible for the clear seasonal cycle and high summer time CCN concentrations observed in the latitude band 45–60°S.

Given these uncertainties concerning the sea spray source function used in previous studies, we investigate in this study how realistically a model using one of the most recent source parametrizations (Mårtensson et al., 2003) reproduces the observed remote marine sea-salt size distributions. We study the emission together with aerosol aging, deposition and cloud interactions in a box model framework. The box model framework includes the University of Helsinki Multicomponent Aerosol model (UHMA) for the aerosol microphysics together with modules for simplified gas phase chemistry, cloud droplet activation, in-cloud chemistry and wet and dry deposition over the ocean. Both in-cloud and below cloud scavenging are considered. In comparison to global model studies, our set-up offers much better control of the simulated system and thus it is able to give more detailed information about the processes that shape the sea salt distribution in the atmosphere. The limitation brought by the use of a box model is that we cannot simulate the effect of entrainment of the aerosols from the FT in detail but must approximate and prescribe the entrained aerosol flux based on earlier studies. We use the model also to study how different environmental conditions, such as wind speed, sea surface temperature and

concentration of DMS in sea water, affect cloud droplet number concentration (CDNC) resulting from the aerosol emissions from the ocean.

2. Method

2.1. The model

The modelling of the marine aerosol is performed using a box-model approach with the aerosol dynamics represented by UHMA model previously described in Korhonen et al. (2004). This box model assumes only one compartment, represented by a well-mixed layer with variable height imitating the marine boundary layer. A flux of aerosol from the FT can be prescribed to simulate entrainment. The aerosol in UHMA is size-segregated and described with 30 logarithmically spaced size sections covering the dry particle diameter range from 20 nm to 17.8 μm. Each size section is assumed to be internally mixed but the model tracks the size-segregated concentration of sulphate and sea salt separately. The basic microphysical processes in the model include condensation, coagulation, dry deposition and nucleation (Korhonen et al., 2004), the latter of which is not modelled in this study.

UHMA has previously been adopted in box model configuration to simulate aerosol mainly over (boreal) continental northern Europe (Korhonen et al., 2004; Grini et al., 2005; Komppula et al., 2006; Tunved et al., 2006). For this study of marine conditions we have modified the model by including sea-salt and DMS emissions, dry deposition of particles over sea, oxidation of DMS to H_2SO_4, and hygroscopic growth of marine particles. The treatment of these new processes is described later.

2.1.1. Emissions and dry deposition. The emission of sea-salt as a function of wind speed, particle size and water temperature was parametrized based on Mårtensson et al. (2003) in the size interval between 0.020 and 2.24 μm D_p. As a significant fraction of sea salt mass is emitted at sizes larger than this range, we described the emission in the size interval D_p 2.24–17.8 μm based on the Monahan et al. (1986) parametrization. The parametrizations overlap well at 2.24 μm. The water temperature dependence of the Mårtensson et al. (2003) source flux is shown in Fig. 1a. The total number of particles emitted is always larger the colder the water is. However, the temperature dependence is different for different parts of the size spectrum. The number of particles emitted at sizes around D_p 100 nm and larger increases when the temperature increases. Figure 1a shows the source fluxes over the whole simulated size range for three wind speeds (5, 9 and 11 m s^{-1}) for a surface water temperature of 9 °C.

Both observations and global model studies have shown that new particle formation in the FT as a result of DMS oxidation, and subsequent entrainment of aerosols formed can act as a source of Aitken mode particles (D_p 20–100 nm) in the marine boundary layer (Clarke and Kapustin, 2002; Spracklen et al., 2007; Korhonen et al., 2008). We cannot describe this phenomenon in detail in a box model, so in some of the simulations we approximate a flux of sulphate aerosols from FT with one of the two functions size distributions shown in Fig. 1a (Raes, 1995; Capaldo et al., 1999). The fluxes shown are for constant FT concentrations of 80 and 400 particles cm^{-3}, assumed to be lognormal distributed centred at 65 nm with a geometric standard deviation of 1.4. The entrainment velocity is set to 0.5 cm s^{-1} (Raes, 1995). Note however, that the entrainment flux is not included into the baseline model simulations.

Emissions of DMS are included in the model as this gas is the natural biogenic source of sulphur in the marine atmosphere. The transfer velocity for DMS from the ocean to the atmosphere as a function of the wind speed is taken from Nightingale et al. (2000). The DMS concentration in surface water is assumed constant throughout each simulation cycle.

For aerosol dry deposition fluxes, the dry deposition velocity parametrization for oceans published by Slinn and Slinn (1980) is used. Dry deposition of DMS and H_2SO_4 is assumed to be zero, while the dry deposition velocity of SO_2 and DMSO is set to 1.1 and 1 cm s^{-1}, respectively (Pham et al., 1995).

2.1.2. Clouds. Cloud and precipitation processes have a large influence on marine aerosol (e.g. Hoppel et al., 1986). In the current approach, a simplified cloud scheme is applied to account for sulphur oxidation as well as in-cloud and below cloud scavenging of aerosol particles. The clouds are intended to represent low-level marine clouds with a depth of 200 m, (the boundary layer height in turn assumed to be 700 m). Thus the cloud processes are applied only to ∼30% (2/7) of the aerosol. This represents the volume of clouds in relation to the volume of the whole box. The frequency of occurrence for clouds is 57%, which is an average for the North Atlantic Ocean (Warren et al., 2006). The updraft velocity for each cloud occasion is assumed constant and its magnitude is determined randomly from the range of 0.08–0.15 m s^{-1}. When the clouds are present they constitute an isolated box apart from the actual mixing layer. When a cloud is about to form, the aerosol in the cloud box is allowed to equilibrate at 99.9% relative humidity. Equilibrating the aerosol at high RH introduces an error when it comes to large, coarse mode particles, (Barahona et al., 2010). This is because the equilibrium size is based on a thermodynamic equilibrium and does not reflect the kinetic limitations which need to be taken into account when large particles/CCN grows. The approximation results in an overestimation of droplet size for coarse mode particles. Droplets larger than 10 um are reduced in size, unrealistic equilibrium sizes of the largest (supermicrometre dry particles) are therefore reduced to a fraction of their size to account for this behaviour; we believe that our approximations are sufficient for the purpose of this study.

The supersaturation is then allowed to increase due to adiabatic cooling resulting from the predefined updraft. Supersaturation above the droplets is determined using regular Köhler theory, resulting in a change in supersaturation depending on the

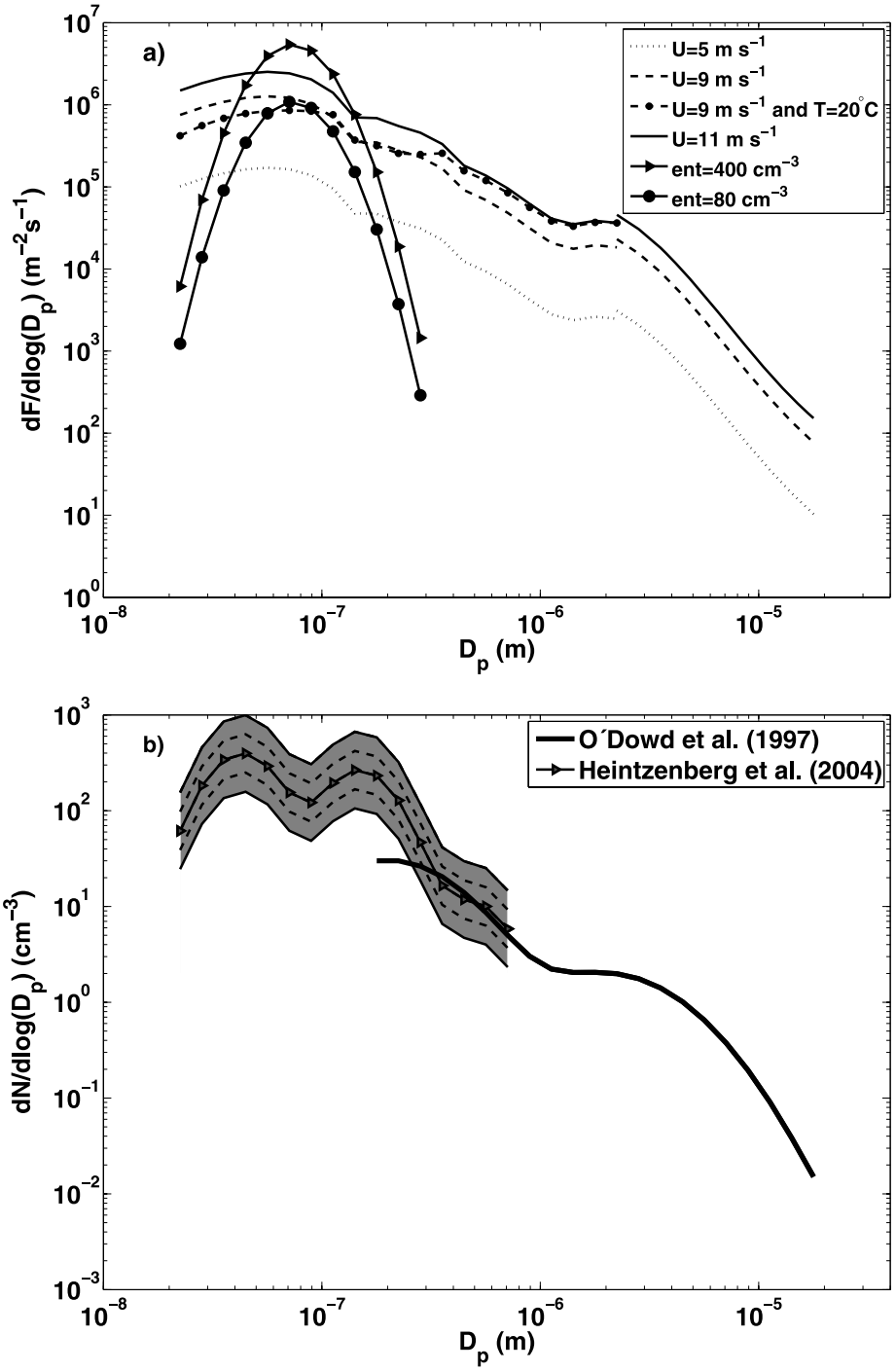

Fig. 1. (a) The number source flux of sea-salt; from Mårtensson et al. (2003) for three different wind speeds in the size interval between 0.020 and 2.24 Em *D*p, the surface water temperature is set to 9 °C, and from Monahan et al. (1986) in the size interval 2.24 to 17.8 Em *D*p. For 9 m s^{-1} is also the emission shown for a surface water temperature of 20 °C; 5 m s^{-1} (dotted curve), 9 m s^{-1} (dashed curve), 9 m s^{-1} and $T = 20$ °C (dashed curve with stars) and 11 m s^{-1} (solid curve). The curves with dots and triangles are entrainment fluxes of a sulphate mode from the free troposphere with a concentration of 80 and 400 particles per cm^{-3}, respectively (Raes, 1995), the entrainment velocity is set to 0.5 cm s^{-1}. (b) Fits to observed marine aerosol number concentrations in the size interval from 100 nm to 17.8 Em *D*p, from O'Dowd et al. (1997), (solid curve), the wind speed is 9 m s^{-1} (only the sea salt) and an average marine size distribution in the interval 20–900 nm *D*p from Heintzenberg et al. (2004) denoted with solid curve with filled triangles, the grey fields shows the probability to find this marine size distribution; inside the dashed lines denotes 0.50 and the total grey field 0.60 probability.

aerosol size distribution. The growth of the droplet population is calculated following Seinfeld and Pandis (1998). The solute is assumed to correspond to sea-salt and sulphate (depending on the simulated composition of the aerosol) assuming a Vant Hoff factor of two and one respectively.

The calculation of clouds does not take into account the effect of ventilation (cloud entrainment), and the water content of the rising air parcel is thus assumed to follow the adiabatic value. The model does not account for the possibility of a broken sky and partial cloud cover and hence indirectly assumes that there is 100% cloud coverage when the cloud is present and 0% coverage otherwise. Once formed, the cloud remains in a static state for 0.5 hours if no precipitation occurs. After 0.5 h, the cloud layer and the remaining mixing layer are mixed and the cloud is recalculated if the model suggests a subsequent cloud. Ideally, the cloud should be completely dynamic. In the current approach, such an extensive treatment is however not possible.

The only dynamic treatment in the cloud once it is formed is coagulation between unactivated particles and activated droplets, which occasionally will have large impact on the number concentration of the smallest particle sizes In this study we choose to omit the coalescence between cloud drops. Although this may lead to changes in the aerosol size distribution, we do not believe that this process can be represented accurately enough given the simplified approach used in the study.

2.1.3. Treatment of in-cloud chemistry. In the bulk of the cloud-water, we allow for oxidation of SO_2 to sulphate by ozone and hydrogen peroxide. The soluble gases (SO_2, NH_3, O_3 and H_2O_2) are partitioned between gas and the bulk liquid phase. The partition is solely based on thermodynamic limitations. The in-cloud oxidation of S(IV) to S(VI) is initialized by calculating the pH of the cloud bulk water, taking into account the liquid water content (LWC), concentration of surrounding gases and the cloud droplet content of sulphate. Once the pH has been established and the equilibrium of reacting gases has been reached, the liquid phase oxidation is calculated. The pH and concentration of reacting gases in the liquid phase is recalculated every time step. We only consider oxidation of S(IV) with hydrogen peroxide and ozone as oxidants according to equations:

$$\mathrm{d[S(IV)O_3]/dt} = [\mathrm{O_3,\ aq}](\mathrm{k0[H_2SO_3]} + \mathrm{k1[HS\ O_{3^-}]} + \mathrm{k2}[\mathrm{SO_3^{2-}}])$$

$$\mathrm{d[S(IV)_{H_2O_2}]/dt} = \mathrm{k_4[H_3O+][HS\ O_3^-][H_2O_2, aq]/(1 + K[H_3O^+)}$$

When the cloud dissipates, the sulphate produced (equivalent amount of sulphuric acid) is distributed over the size range of activated particles according to the individual water content of each droplet. This approach represents a simplification of the representation using droplet specific chemistry, and the bulk value may not be representative for all particle size classes. This is due to the fact that the composition and size of the individual particles typically vary, and both the reaction rate in these droplets as well as the total amount of oxidized sulphur may differ from the value derived for the bulk. However, this simplification is believed sufficiently accurate with respect to the scientific goal of the study.

2.1.4. Wet deposition. The frequency of rain events is statistically prescribed (60% of the cloud events) and the precipitation intensity varies between moderate (0.2 mm d^{-1}) and heavy drizzle (1.0 mm d^{-1}). Both rainout (removal of cloud droplets from the cloud due to precipitation formation) and washout (i.e. below cloud scavenging of aerosols) is accounted for. The fraction of activated droplets that are removed is determined from the precipitation rate, cloud height and LWC of the cloud. Based on the LWC and height of the cloud, column LWC is estimated. From this information we estimate the fraction of the cloud that rains out during a precipitation event, and in turn this is directly translated to removal rate of aerosols, assuming the same removal rate for all size classes of the activated droplets. In order to maintain realistic cloud properties during rain events, no more than 40% of the population of activated particles are removed from the cloud. Once this threshold is reached, the cloud layer and mixing layer is mixed and the cloud recalculated. Since we use a static cloud, this approach is necessary to maintain reasonable rainout efficiencies. Below cloud scavenging coefficients are taken from an empirically based parametrization by Laakso et al. (2003) that relies on precipitation intensity and particle size. Due to the characteristics of the measurements used to develop this parametrization, it is valid only for particle size range 20 nnm $< D_p <$ 510 nnm. The scavenging coefficients are extrapolated to account also for particles with size ranging from 0.510 to 2.0 μm D_p.

2.1.5. Gas phase chemistry. The chemistry scheme included in the model utilizes a simple steady-state approach for calculating the concentrations of hydroxyl and nitrate radicals (Tunved et al., 2006). The concentration of OH is determined assuming balance between formation and degradation of odd hydrogen (HO_x = OH, HO_2). HO_x is generated by reaction of O^1D and water vapour. The sinks of odd oxygen are HO_2-HO_2 self-reaction, OH-HO_2 reaction and formation of nitric acid from a combination of OH and NO_2.

Nitrate radical is formed from the reaction of NO_2 and O_3. The model is initialized with typical sulphur dioxide, ozone and NO_x mixing ratios for the remote marine taken from Seinfeld and Pandis (1998). The daytime length is assumed as 12 h. For the oxidation of DMS to SO_2 and DMSO, DMSO to SO_2 and finally SO_2 to H_2SO_4, the rate coefficients from Pham et al. (1995) are used.

2.2. Basic model set-up

We initialize the model gas concentrations with mean values for the remote marine environment taken from Seinfeld and Pandis (1998) and presented in Table 1. The DMS concentration in the

Table 1. The initial gas concentrations (in ppbv) used for the model

O_3	NO_2	NO	O_2	N_2	HCHO	CH_4	CO	SO_2	DMS
25	0.026	0.0062	0.23×10^9	0.7×10^9	0.8	1.72×10^3	100	0.02	0.1

sea water is taken to be the annual global mean of 1.8 nmol dm^{-3} (Kloster et al., 2006). These values can be considered to represent average remote mid-latitude (temperate) marine conditions.

The aerosol model is allowed to spin up from zero concentration for 332 h (14 d) and then run for additional 268 h (11 d) to generate a period of data to be used for further analysis. Using a long spin-up time minimizes the effects of the zero initialization, and allow the aerosol to approach steady state conditions, although the cloud cycles still cause large variability.

We will compare the simulated size distributions to the measurements presented by O'Dowd et al. (1997) (Fig. 1b), which the authors claim to represent a typical size distribution for the sea-salt fraction of the marine aerosol in a clean remote North Atlantic Ocean boundary layer. These measurements were made in September, when the effect of DMS or organic compounds on the size distribution is not expected to be very strong. For the comparison with these observations, the modelled sulphate fraction is removed from the aerosol and the corresponding sea-salt radii are recalculated. This is an approach designed to simulate the measurement technique where particles are heated to 300 °C, as in O'Dowd and Smith (1993), the temperature at which the semi-volatile fraction disappears, and the obtained size distribution consists of only sea-salt. Mineral dust and soot also have low volatility and can remain in the aerosols at 300 °C but they are only found in aerosols influenced by continental and anthropogenic sources and have little influence on the remote marine aerosol. Furthermore, to allow comparison with the measurements reported in O'Dowd et al. (1997) the meteorological parameters are set to following values: wind speed 9 m s^{-1}, surface water and air temperature 9 °C and relative humidity 90%. No size resolved measurements of the sea-salt fraction in the marine aerosol are available for particles smaller that 100 nm D_p, instead the average size distribution from four experiments presented in Heintzenberg et al. (2004) will be used for a comparison in the size interval 20 and 700 nm D_p. This fit to data represents the aerosol in the pristine marine environment; only data with back trajectories of at least 120 h without land contact have been used. The chemical composition of this submicrometre remote marine aerosol is not given in Heintzenberg et al. (2004), with the exception of the mode centred at 700 nm D_p which is assumed to be sea-salt. Also no meteorological parameters associated with the measured distributions are available and therefore the first comparison will be with the base case simulation. The values given here are for the base case simulation. For all other simulations, we use these same values unless indicated otherwise.

3. Results

3.1. Base case simulation

3.1.1. Comparison of base case model results to observations. Figure 2 shows the modelled total number concentration during the base case run together with the simulated DMS (mean 0.274 ppbv), SO_2 (mean 0.023 ppbv) and H_2SO_4 (mean 1.1×10^7 cm^{-3}), all of which are within the range of measured concentrations in the marine boundary layer (Weber et al., 2001; Aranami et al., 2002; Berresheim et al., 2002). The predicted mean model number concentration 200 ± 43 cm^{-3} is in the range of measured number concentrations of remote marine aerosols, 284 ± 107 cm^{-3} in the size range 20–500 nm D_p during ACE-1 (Bates et al., 2000), and 150–300 cm^{-3} in the size range 0.012–1.04 μm D_p in the trade wind region (Hoppel and Frick, 1990). The modelled CDNC is 39 ± 16 cm^{-3}, which is in the range of measured CCN concentrations in clean air masses, 27 ± 8 and 42 ± 14 cm^{-3} for cloudy and clear conditions, respectively by Chuang et al. (2000), who measured at a supersaturation of 0.1%. In the model the supersaturation changes according to the Köhler theory, depending on up draft, number concentration and size distribution. However, the mean supersaturation is the same as used in the measurements, i.e. 0.1%. The simulated variability in the number concentration (Fig. 2) is due to the presence of clouds and the amount of precipitation. The mean modelled LWC content is 0.18 g m^{-3}, within the range of observed values (Seinfeld and Pandis, 1998).

Figure 3 shows a comparison between the median sea salt aerosol number distribution from the base case and the fit to measured number concentration according to O'Dowd et al. (1997) and Heintzenberg et al. (2004). Good agreement can be seen in the 0.3–2.2 μm D_p size range which indicates that the Mårtensson et al. (2003) emission parametrization is consistent with measurements in this size interval, when applied at the same conditions as those that prevailed during the O'Dowd and Smith (1993) observations. For particles larger than 2.2 μm in diameter (described with Monahan et al. (1986) parametrization) the simulation gives lower than observed concentrations and over the size range of 200–300 nm D_p the median concentrations are high compared to those observed by O'Dowd et al. (1997). Particles including both sea-salt and sulphate smaller than 300 nm D_p are validated with Heintzenberg et al. (2004). The simulated and measured medians are not the same, but the simulated numbers show a high probability of being found close to the observations over most of the size range.

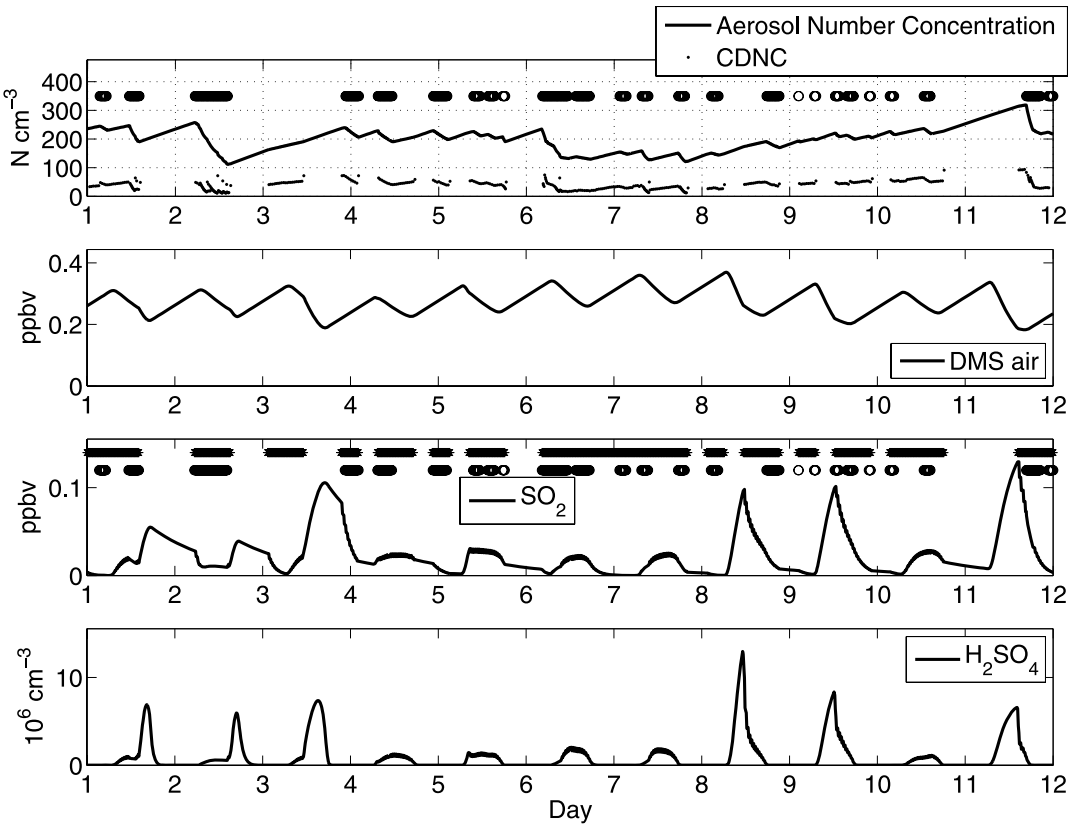

Fig. 2. Total aerosol number concentration and CDNC, DMS, SO_2 and H_2SO_4 concentrations as time series for the 11-d base case simulation. The stars at the top of the plots indicate when clouds are present and the circles denote when it is precipitating.

It is important to note that any agreement or disagreement of our modelled results with the observations cannot be taken as a full validation of the sea spray source flux in a certain size range, although the probability distribution function of Heintzenberg et al. (2004) is of some use in this regard. The Heintzenberg et al. (2004) data is based on a large set of measurements and compared to that the simulation show a good agreement, but still the chemical composition has not yet been fully validated, at least not for the Aitken mode. The size distributions given in O'Dowd et al. (1997) are averages of measurements made over a limited period of time, and we do not have detailed information of the cloud and precipitation conditions encountered prior and during the measurements. What the good agreement of the modelled and measured size distributions shows, however, is that the Mårtensson et al. (2003) parametrization provides a source function that results in a sea-salt number size distribution that is not significantly different from the O'Dowd et al. (1997) parametrization in the size range 0.3–2.0 μm D_p. The total aerosol number size distribution is typical for the remote marine boundary layer (compare with Bates et al., 2000; Heintzenberg et al., 2000) with a reasonable total mean and median aerosol number concentration (200 and 206 cm^{-3}), a pronounced Hoppel-minimum and an Aitken and accumulation mode with a high probability to be found over the ocean according to Heintzenberg et al. (2004).

The modelled sea-salt and sulphate mass are compared with three measurements made in remote marine environments (QUEST-1, ACE-1 and ACE-2 campaigns). It is unrealistic to expect exact agreement between model and observations as the average water/air temperature, boundary layer height, DMS concentration and wind speed during the three campaigns were not exactly the same as in the base case simulation. These parameters have most probably changed during the transport of the accumulation mode (0.1–1.0 μm D_p) particles to the measurement site as the accumulation mode particles can have a life time of up to 5 d if there is no wet deposition; however, the comparison provides a way to qualitatively assess how realistically the model simulates aerosol sources and aging in a remote marine atmosphere, and since the measured wind speeds are not known, this is the best we can do.

The sampling methods used during the campaigns were as follows: during QUEST-1 (Cavalli et al., 2004) seven stages of an eight stage low-pressure Berner impactor were used; the upper cut off diameter was 8 μm. During ACE-1 and ACE-2 (Quinn et al., 2000) a seven-stage multijet cascade impactor with a 10 μm cut off diameter was used. During QUEST-1 the humidity

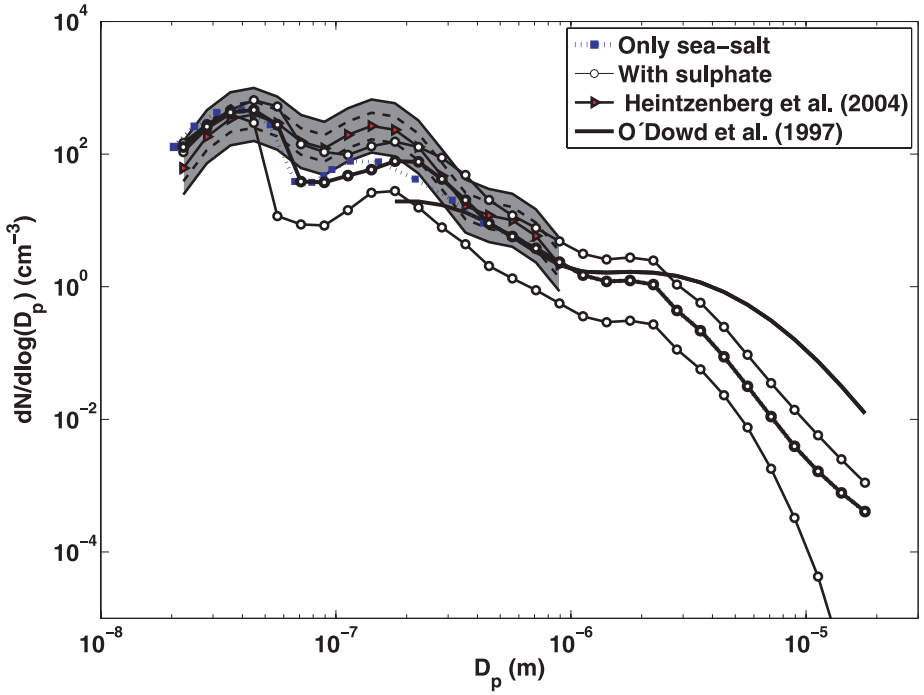

Fig. 3. Comparison between the base case simulation (median over 11 d) and measured size distributions (from O'Dowd et al. (1997) denoted with solid curve and Heintzenberg et al. (2004) denoted with solid curve with filled triangles, the greay fields shows the probability to find the size distribution, inside the dashed lines denotes 0.50 and the total grey field 0.60 probability). The model was run with the wind speed at 9 m s^{-1}, the water temperature 9 °C and the DMS concentration in the water 1.8 nmol dm^{-3}. The dotted curve with squares is the modelled aerosol, containing only the sea-salt fraction (sodium chloride) and the solid curves with circles shows the size distribution when the both sulphate and sea-salt remains in the aerosols, (median number concentrations and 5 and 95 percentiles, the thinner curves for the percentiles).

was 80 ± 8% and 55% during ACE-1 and ACE-2. The comparison shows the measured submicrometre and supermicrometre masses (classification based on aerodynamic diameter) where a cut-off between the two subsets is 1 μm D_p for QUEST-1, and 1.1 μm D_p for ACE-1 and ACE-2. To be able to compare the modelled and the measured aerosol mass, the measured particle sizes are recalculated to dry diameters and the modelled geometric diameters are recalculated to aerodynamic diameters (the density is set to 2 g cm^{-3}), but there remains small differences in the size cuts.

The sulphate and sea-salt mass concentrations from the model show good agreement with measurements both in the size range below 1 μm and for the particles larger than 1 μm (Table 2). Best agreement is found for modelled masses compared with ACE-1, where most masses are within the range of the measurements, apart from in the submicrometre sea salt range where the mass is smaller in the model. The measurements during ACE-1 were performed in the southern hemisphere where the influence of anthropogenic sources is expected to be small. The agreement with the other campaigns is also good. One reason for the higher mass concentrations during QUEST-1 could be higher wind speeds over the Atlantic Ocean during the transport to Mace Head. Another problem with the comparison is that the submicrometre particles contained a large fraction of organics (Cavalli et al., 2004), and this source is not yet included in the model.

3.2. *Sensitivity of simulated aerosol properties to key model parameters*

We now examine how the simulated results depend on model input parameters, such as sea surface water temperature (T_w), wind speed and DMS surface water concentration. In the sensitivity simulations the atmospheric conditions (e.g. gas concentrations) and the cloud parameters, (cloud depth, frequency of occurrence, updraft and precipitation) are the same as during the base case simulation. Our aim is to test the sensitivity of the system and the importance of different processes, including clouds, precipitation and atmospheric conditions, on the modelled aerosol properties. We will also investigate whether the O'Dowd et al. (1997) parametrization can be applied outside its initial observational conditions, which were used in the base case simulation. Questions that will be addressed in the discussion below include: How will sea-salt and sulphate be distributed over the size spectra? How important are the clouds and precipitation, the water temperature, DMS emission, entrainment and wind speed on the final aerosol number size distribution and CDNC? How will the

Table 2. Masses of sea-salt and sulphate for the base case simulation compared with measurements from three campaigns. The sizes of the particles from the model are recalculated to dry aerodynamic diameter; the values in the brackets are the original geometric mean diameter in the size bin. From the measurements is it the cut-off diameter and; the values in the brackets are the wet particle diameter

Reference	Sulphate μg m^{-3}	Sea-salt μg m^{-3}
Model base case corrected to aerodynamic diameter (density 2.0 g cm^{-3})	$D_p < 0.63$ (0.45) μm	$D_p < 0.63$ (0.45) μm
	0.20	0.26
	0.63 μm $> D_p >$ 5.0 (3.6) μm	0.63 μm $> D_p >$ 5.0 (3.6) μm
	0.02	5.9
QUEST-1 (Cavalli et al., 2004)	$D_p < 0.55$ (1.0) μm	$D_p < 0.55$ (1.0) μm
	0.26 ± 0.04	0.39 ± 0.08
	0.55 μm $> D_p >$ 4.4 (8.0) μm	0.55 μm $> D_p >$ 4.4 (8.0) μm
	0.030 ± 0.01	10.16 ± 0.80
Model base case corrected to aerodynamic diameter (density 2.0 g cm^{-3})	$D_p < 0.8$ (0.56) μm	$D_p < 0.8$ (0.56) μm
	0.21	0.38
	0.8 μm $> D_p >$ 8.0 (5.6) μm	0.8 μm $> D_p >$ 8.0 (5.6) μm
	0.015	7.6
ACE-2 (Quinn et al., 2000)	$D_p < 0.83$ μm (1.1 μm)	$D_p < 0.83$ (1.1) μm
	0.68 ± 0.17	0.60 ± 0.51
	0.83 μm $> D_p >$ 7.6 μm	0.83 μm $> D_p >$ 7.6 μm
	0.15 ± 0.03	6.3 ± 1.6
ACE-1 (Quinn et al, 2000)	$D_p < 0.83$ μm	$D_p < 0.83$ μm
	0.16 ± 0.06	1.0 ± 0.55
	0.83 μm $> D_p >$ 7.6 μm	0.83 μm $> D_p >$ 7.6 μm
	0.07 ± 0.09	9.4 ± 5.5

mass concentrations of sea-salt and sulphate change when these parameters are varied?

3.2.1. Effect of surface water temperature. As seen in Fig. 1a, the shape of the sea spray source function of Mårtensson et al. (2003) is dependent on seawater temperature. For example, when the water temperature increases from 9 to 20°C, there is a clear increase in the flux of particles $D_p > 100$ nm, but a decrease in the ultrafine particle source. The latter of these effects dominates the total number flux, and as a result, the total sea-salt particle number emission flux at 2 °C is 31% larger than at 20 °C. This dependence feeds also into the simulated size distribution properties, but not directly, as is evident from Fig. 4. The initial negative number flux trend with increasing temperature seen in the source parametrization survives only below ∼40 nm D_p, whereas in the source function the effect of temperature is evident up till 100 nm D_p. The magnitude of the effect in the ultrafine size range is also smaller in the simulated size distribution than in the source function. For particles larger than ∼250 nm D_p, however, the positive trend in the number source flux with increasing temperature is clearly seen in the simulated size distribution, with a magnitude very similar to the source function temperature dependence. The size range in between these two regions, including important parts of the Aitken and accumulation mode particles, has a less clear temperature dependence.

The effect of sea surface water temperature on the marine aerosol number and CDNC are shown in Fig. 5a and b for six different temperatures, together with 5 and 95 percentiles. Most of the variability results from wet deposition, which we will examine in detail below. The variability of both aerosol and CDNC is largest for the cold waters. In the case of aerosol number (Fig. 5a), the highest average concentration is found at 12 °C with 201 particles cm^{-3}. When the temperature increases from 12 to 20 °C the average aerosol number concentration decreases by 23% to 163 particles cm^{-3}. For the CDNC (Fig. 5b), the change is smaller and of opposite sign than in the aerosol number concentration. The change in CDNC is small for temperatures larger than 9 °C, but there is an increase of CDNC when the temperature increases from 2 to 9 °C.

3.2.2. Effect of DMS emission. Oceanic DMS concentrations have a high temporal (higher production in summer than winter) and spatial variation (higher production in biologically active regions). To account for this variability we have in the model varied the DMS concentrations in the surface water from 0.0 to 20.0 nmol dm^{-3}. All parameters, e.g. temperature, wind speed and clouds, apart from the DMS concentration are the same as in the base case.

In Fig. 6a, the average size distributions resulting from three DMS concentrations are shown. Without any DMS source, and in the absence of anthropogenic sources and entrainment, the

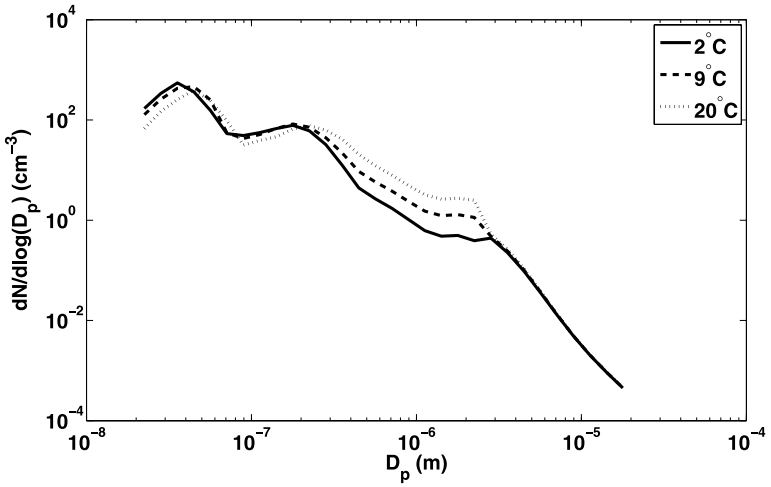

Fig. 4. Size distributions from simulations with three different water temperatures, the lines show the total (with both sulphate and sea-salt in the aerosols) mean size distribution from model runs with a wind speed of 9 m s^{-1} and a DMS concentration of 1.8 nmol dm^{-3}. The water temperature is set to 2 °C (solid curve), 9 °C (dashed curve) and 20 °C (dotted curve).

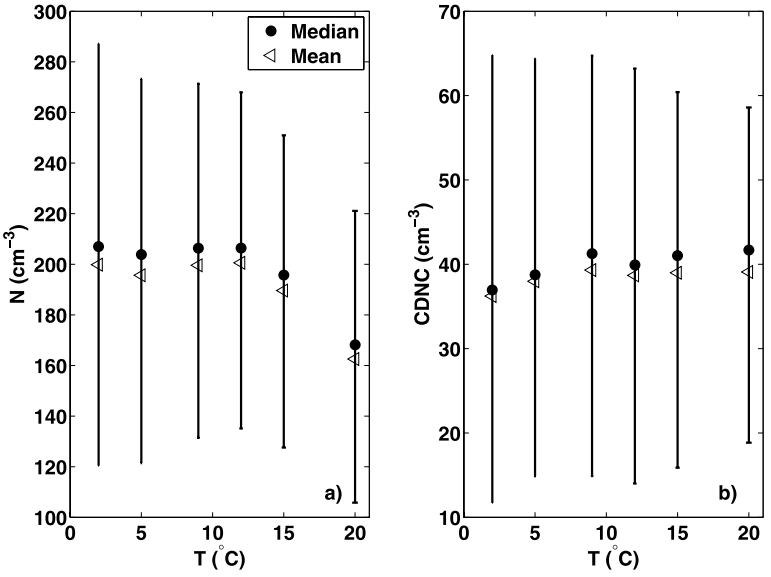

Fig. 5. (a) The average number concentrations from model runs with different water temperatures; mean concentration (triangles), median concentration (dots) and 5 and 95 percentiles (bars). (b) As (a) but for the CDNC activated according to Köhler theory.

resulting average size distribution consists only of sea salt from the sea spray source function and the sink processes and therefore resembles much of the shape of the sea salt source function in Fig. 1a. For both low (1.8 nmol dm^{-3}) and high (20 nmol dm^{-3}) DMS water concentrations, we can see much more pronounced Aitken and accumulation modes, mainly as a result sulphate formation in activated cloud droplets. At high DMS concentrations, condensation of sulphuric acid also clearly grows the Aitken mode sea spray particles to cloud droplet sizes. The best agreement with O'Dowd et al. (1997) in the range 200–400 nm D_p are for the simulation without a DMS source. This suggests a very low DMS source during the O'Dowd et al. (1997) cruise.

When the DMS concentration in the water is set to 1.0 nmol dm^{-3}, the size distribution for $D_p < 1.0$ μm is similar to the distribution from Heintzenberg et al. (2004), Fig. 6b. Particles down to 50 nm D_p have been activated to cloud droplets, showing the importance of Aitken mode particles in marine cloud formation. The accumulation mode is also comparable with Heintzenberg et al. (2004), even if simulated median number concentration is lower than the measured in the size interval influenced by cloud processes, $45 < D_p < 360$ nm. For the smallest and larger particles the simulated concentration is close to, but somewhat higher than the measured median concentration.

Figure 7a shows the medians, 5 and 95% percentiles and means for the total number concentration for seven different prescribed DMS concentrations. The aerosol number concentration increases by 5% when the DSM increases from 0.0 to 4.0 nmol dm^{-3}. However, as the DMS concentration continues to increase, the number concentration decreases by 9% indicating the possibly existence of a peak number concentration at ~4.0 nmol dm^{-3}, although the total concentration never deviates more than 10% from the value of ~190 cm^{-3} at zero DMS emissions. There is also a weak relationship between the average of CDNC and the DMS concentration. Maximum CDNC is found at

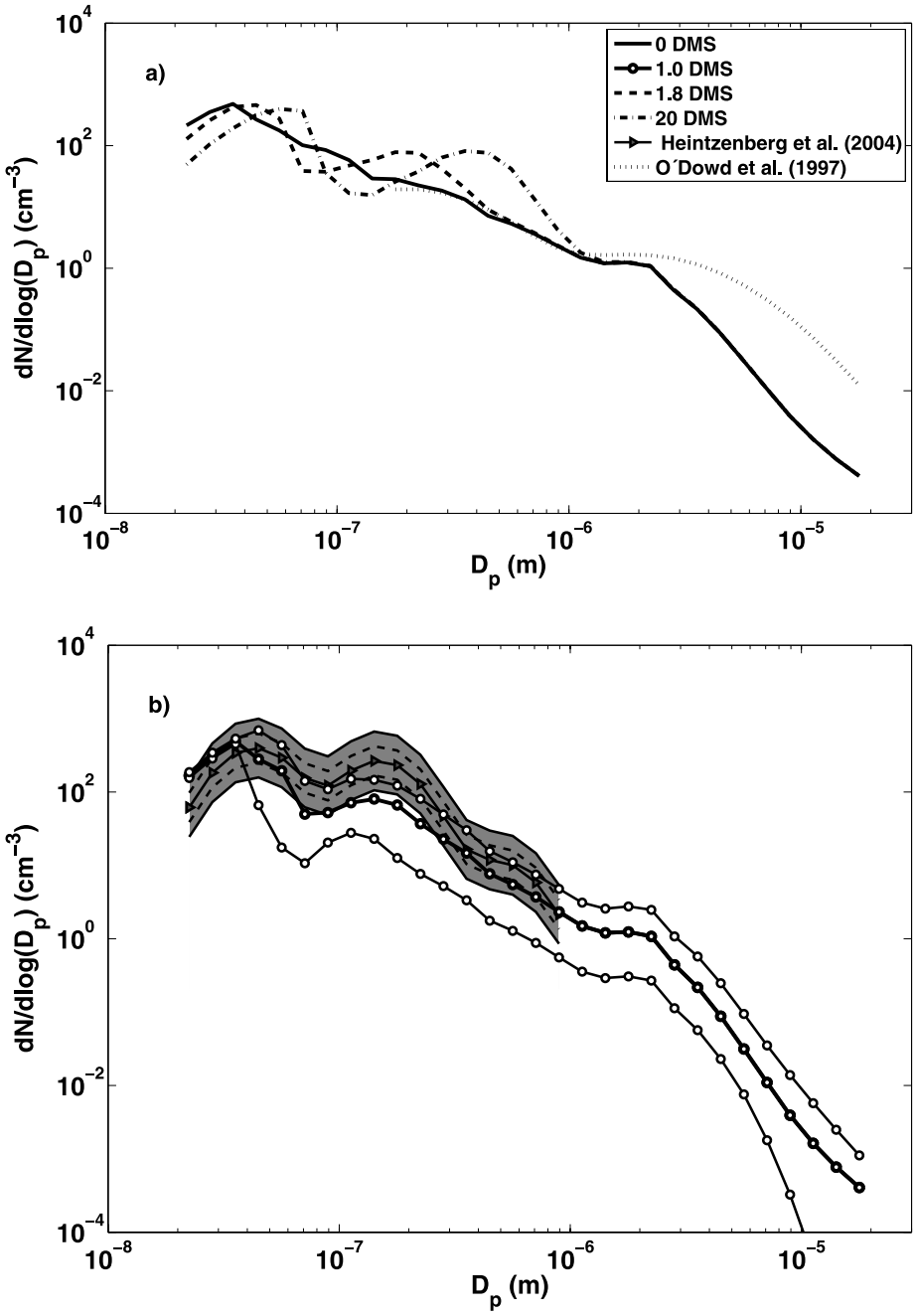

Fig. 6. (a) Size distributions from simulations with three different DMS concentration in the water, the lines show the total (with both sulphate and sea-salt in the aerosols) median size distribution from model runs with a wind speed of 9 m s^{-1} and a temperature of 9 °C, the DMS concentration is 0 nmol dm^{-3} (solid curve), 1.8 nmol dm^{-3} (dashed curve) and 20 nmol dm^{-3} (dash–dotted curve). Included is also the sea salt concentration parametrized by O'Dowd et al. (1997) (dotted curve). (b) Size distributions for the total (with both sulphate and sea-salt) aerosol from simulations with a DMS concentration of 1.0 nmol dm^{-3} (solid thick curve with circles represent the median concentration and thinner curves with circles the 5 and 95 percentiles). Model runs with a wind speed of 9 m s^{-1} and a temperature of 9 °C. Included is also the concentration parametrized by Heintzenberg et al. (2004) denoted with solid curve with filled triangles, the grey fields shows the probability to find this marine size distribution, inside the dashed lines denotes 0.50 probability and the total grey field 0.60 probability.

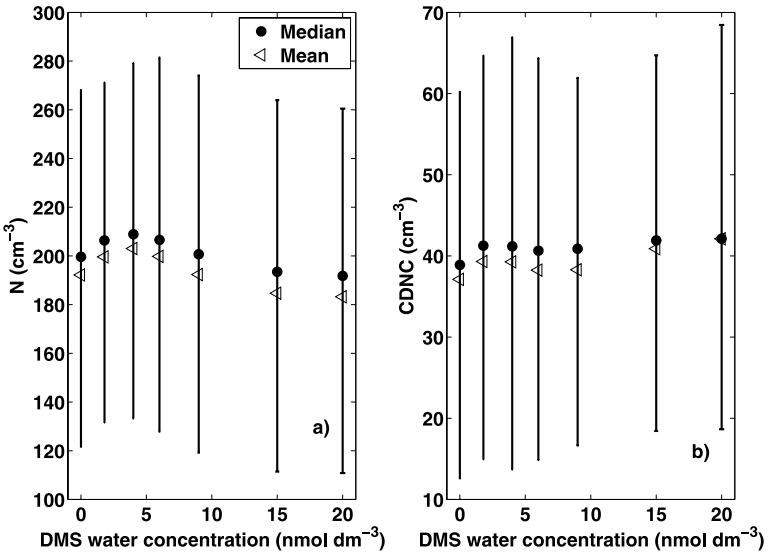

Fig. 7. (a) The average number concentration from model runs with different DMS concentration; mean concentration (triangles), median concentration (dots) and 5 and 95 percentiles (bars). (b) As (a) but for the CDNC activated according to Köhler theory.

20 nmol dm^{-3}, which is 13% higher than at 0.0 DMS. Between these two extremes in DMS concentration, there is no clear trend in CDNC. The reasons for the relatively small differences in CDNC, despite the clear changes in the accumulation mode particle concentration, are discussed in Section 4.4. It is also important to note that we do not explicitly simulate the effect of DMS on nucleation in the FT and thus we may underestimate the sensitivity of the results to DMS flux on longer time scales. Models which include both the boundary layer and the FT, for example the 3-D model by Korhonen et al. (2008) show that the effect of DMS emissions on the CCN number is non-local due to the long time it takes for the emissions to convert into nanometre sized nuclei and then grow to CCN sizes. This is in agreement with the fact that nucleation in the marine boundary layer is very rare. Note however that the new particle formation in the FT in our simulations is indirectly included when we test the effect of entrainment, see later.

3.2.3. Effect of clouds and precipitation. Clouds have a potential to influence the aerosol size distribution in several ways. The aerosols that activate as cloud drops can grow in size by aqueous phase oxidation of sulphur or, if precipitation forms, be scavenged from the atmosphere. Precipitation reduces the aerosol number concentration also below the cloud. Interstitial aerosols inside the cloud can be scavenged by coagulation into large cloud or rain droplets. To investigate the effect of clouds and precipitation on the marine aerosol size distribution, we firstly consider a situation when no clouds and no precipitation are included (Fig. 8). This may not be a realistic case, but is

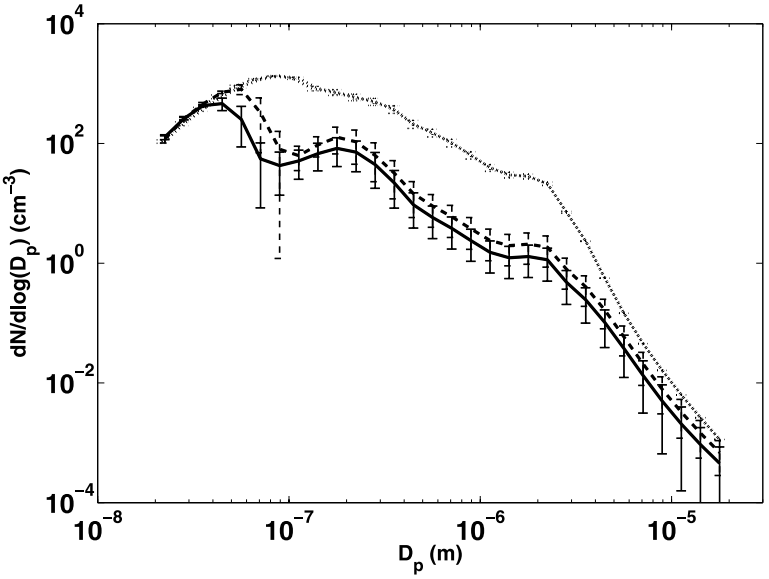

Fig. 8. The aerosol concentration modelled near steady state without any cloud processes (dotted curve) and the total aerosol concentrations (both sulphate and sea-salt) for the base case simulation (solid curve) with 26% rain frequency and a simulation with 11% rain frequency (dashed curve). The variations are shown with the bars for the 25 and 75 percentiles. The model runs were made with a wind speed of 9 m s^{-1}, temperature of 9 °C and DMS concentration of 1.8 nmol dm^{-3} in the water.

helpful in order to isolate the cloud and precipitation effect. Clearly, when no clouds are included, the model overpredicts the sea salt number concentration in the size range ∼50 nm to ∼4 μm D_p by approximately an order of magnitude compared to what is typically found over the oceans and shown in the base case simulation. The maximum difference is found just below 100 nm D_p, in the size range that usually shows a minimum due to cloud droplet activation. As expected, below the typical size range for smallest cloud activation diameter, the number concentration is not strongly affected compared to the base case. To achieve a strict steady state condition without clouds, one needs to run the model for an unrealistically long time because in the absence of wet sinks the aerosol turn over time depends only on the relatively weak dry deposition. This increases the time required for the model to approach steady state. Figure 8 also shows that a lower rain frequency of 11% produces the same features as the 26% case, but that the Aitken mode is larger and the total concentration is higher, due to less precipitation and larger activation diameter for the cloud droplets (see Section 4.4.).

3.2.4. Effect of entrainment from FT. In the remote marine boundary layer, entrainment of aerosols from FT is typically a source of Aitken mode sized sulphate particles that have formed at higher, and thus colder, altitudes. Figure 9 compares the resulting average number size distribution for the base case (no entrainment), and low and high entrainment (compare also Fig. 1b). It is clear that the source of Aitken mode particles from the FT by entrainment influences the number concentration between 30 and 300 nm D_p. The total number concentrations increase by 28% assuming the smaller source and by 134% assuming the higher source, and the respective CDNC increase by 12 and 59%. Although our approach to model new particle formation and entrainment from FT is simplified and involve uncertainties reflected also in the results, still it is evident that if episodes of new particle formation in the FT take place, the subsequent transport down to the MBL can have a potential to strongly influence the size distribution and cloud droplet properties of the MBL aerosol.

3.2.5. Effect of wind speed. Wind speed affects the aerosol size distribution through source fluxes of sea-salt particles and DMS. Figure 10 shows the change in the average number size distribution for the total aerosol with changing wind speed and Fig. 11 shows how the resulting average total number concentration and CDNC depend on the wind speed. Based on our simulations we find for the total number concentration a dependence $\mathrm{Log}(N) = 0.25\mathrm{U} + 0.01$, which is somewhat different from the one found in the measurements of Nilsson et al. (2001) [they observed $\mathrm{Log}(N) = 0.10\mathrm{U} + 1.6$]. Their observations were however in the presence of an Aitken mode uncorrelated to the wind speed and there may have been long range transported or entrained aged anthropogenic aerosols. In real atmospheric data, unlike in our model, there are almost always other aerosol sources present to some degree, which will decrease the slope and add to zero bias. For CDNC we obtain a wind speed dependence of the form $\mathrm{Log(CDNC)} = 0.16\mathrm{U} + 0.14$.

4. Discussion

4.1. Influence of key parameters on aerosol number concentration and CDNC

Our sensitivity simulations show that the effect of water temperature on the sea spray source, as shown in Fig. 1a, is not fully transferred into the marine size distribution in the ultrafine particle range, although a slight temperature effect is seen for particles smaller than 40 nm. On the other hand, the water temperature does affect the concentration of sea salt particles >250 nm D_p, and thus the airborne sea salt mass, significantly. As this size range contains low aerosol number, however, the total number concentration (which is shown in Fig. 5a and dominated by the Aitken mode particles) shows a decline from temperate to tropical temperatures. For the ultrafine size range the

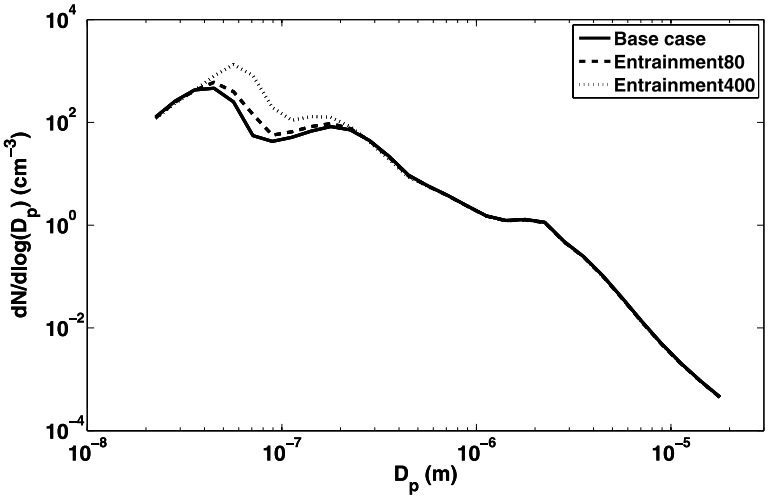

Fig. 9. Effect of entrainment of aerosols from the free troposphere (FT), the lines show the total (with both sulphate and sea-salt in the aerosol) mean size distribution from model runs with a wind speed of 9 m s^{-1}, temperature of 9 °C and DMS concentration of 1.8 nmol dm^{-3} in the water. Shown are the base case with no entrainment (solid curve), FT aerosol concentration of 80 cm^{-3} (dashed curve) and 400 cm^{-3} (dotted curve).

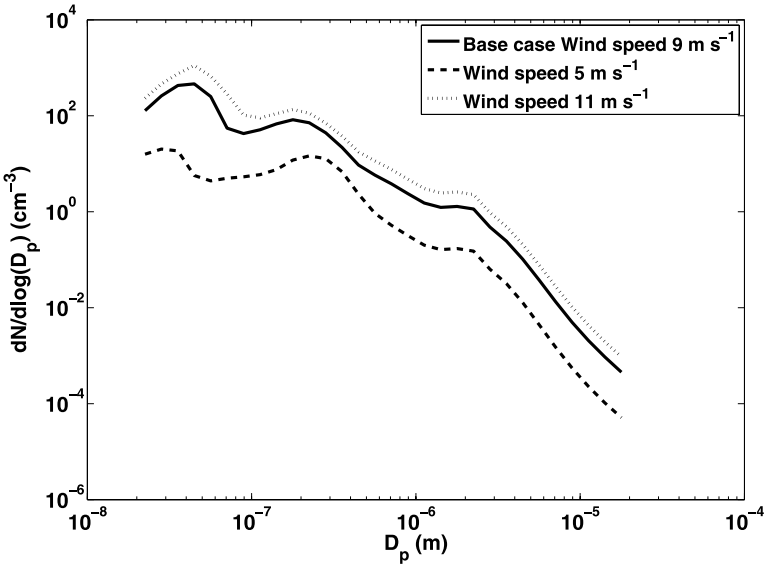

Fig. 10. Size distributions for three different wind speeds. The lines show the total (with both sulphate and sea-salt in the aerosol) mean size distribution from model runs with a water temperature of 9 °C and a DMS concentration of 1.8 nmol dm^{-3}. The wind speed is 5 m s^{-1} (dashed curve), 9 m s^{-1} (solid curve) and 11 m s^{-1} (dotted curve).

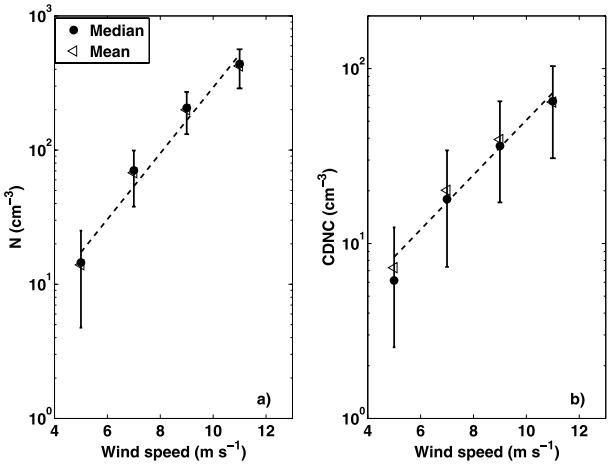

Fig. 11. (a) The average number concentration from model runs with different wind speeds; mean concentration (triangles), median concentration (dots) and 5 and 95 percentiles (bars), the dashed line represent the best fit to data. (b) As (a) but for the CDNC activated according to Köhler theory.

effect of temperature through the source flux is cancelled out by other processes that shape the aerosol size distribution in the marine environment.

It is noteworthy that especially in the size range of 50–250 nm D_p, where highest CDNC is found, shows weak temperature dependence when we look only at the average CDNC. This is not, however, true concerning the aerosol concentration, or the CDNC from sea spray >250 nm D_p. The median CDNC increase slightly more (from 37 to 42 cm^{-3}) going from Arctic to tropical temperature, which indicates that the distribution is near normal at low temperature and somewhat skewed at high temperature (remember that we use the same random sequence to drive the simulations) compared to low temperature, see Fig. 5b. The effect on the CDNC from temperature is smaller than what was shown by Pierce and Adams (2006), and our tests suggest that the difference is due to how CDNC are calculated: in our case we use a full Köhler activation to determine supersaturation, critical diameter and the CDNC, while Pierce and Adams (2006) activated every aerosol larger than a certain fixed diameter. Exactly how the CDNC production is affected by sea surface temperature will most likely vary with season and climate zone and their combined temperature patterns, which will require a more detailed model than ours.

Even less changes occur in the total CDNC due to changes in DMS emissions, see Fig. 7. This indicates that the effect of DMS on marine CDNC is not through growing ultrafine sea spray particles to cloud active sizes, but through formation of new particles in the FT. The effect is expected to strongly affect of the CDNC in areas of entrainment, whereas without entrainment and in biologically non-active seasons the wind speed appears to be the dominant key parameter for the CDNC as well as aerosol number concentration.

4.2. *The marine aerosol sources*

The submicrometre sea salt distribution, which itself has no Aitken and accumulation modes (Fig. 6), acts as a backbone for the typically observed marine aerosol distribution. Even a modest DMS source leads to physical and chemical processes (condensation and especially cloud processing giving rise to Hoppel minimum), which grow a bimodal distribution on this backbone. It is interesting to note that neither DMS driven nucleation in the BL nor entrainment from FT is necessary for the formation of these two modes. As entrainment has, however, been shown by

previous observations (Clarke and Kapustin, 2002) and global model simulations (Spracklen et al., 2007) to provide a source of Aitken mode particles into the MBL, it remains for future studies to find out its relative contribution to the submicrometre marine aerosol now when the sea spray has been established as an alternative source. A fraction of the submicrometre marine aerosol has been found to consist of organics, (e.g. Middlebrook et al., 1998; Cavalli et al., 2004; Leck and Bigg, 2005a;b; Russell et al., 2010), the latter with a parametrization for the organic mass as a function of the wind speed, but no parametrizations are available yet for the size resolved organic fraction.

We have shown that the inclusion of a realistic sea spray source offers a possible explanation to the typically observed remote marine submicrometre aerosol distribution that had not been obvious from previous model studies and renders it unnecessary to try to explain the production of marine CDNC by the rarely observed nucleation events or by the introduction of entrained aerosols, although the latter is probably of regional importance. Despite numerous studies, nucleation has only rarely been observed over the oceans (Clarke et al., 1998), and is in most cases absent (Bates et al., 2000) except over the ice covered Arctic ocean (Wiedensohler et al., 1996), where the ice is an efficient lid preventing local sea spray formation (Nilsson et al., 2001). This has lead several investigators to propose entrainment from the FT as the only possible source for remote marine CDNC (e.g. Raes, 1995; Clarke et al., 1996). None of these studies included submicrometre sea spray in their models; simply because it was believed that sea spray consisted solely of supermicrometre particles. Here we demonstrate that submicrometre together with the ultrafine sea spray offers an alternative source.

4.3. *The essential importance of clouds and precipitation*

Figure 8 demonstrates the importance of cloud and precipitation and the sink processes associated with them in balancing the aerosol sources and therefore simulating a realistic remote marine aerosol concentration. As a measure of this, one can consider the long time period (∼2000 h) needed to reach a steady state between sources and dry deposition (and coagulation) without any wet sinks. Total absence of wet sinks results in significantly too high aerosol concentrations. In practise, such a large number implies that the marine aerosol would never be in steady state through dry deposition alone. On all oceans, some precipitation or cloud processing will have occurred over such a long time span. We can also see that in the range below 3 μm D_p, the aerosol number concentration is overpredicted compared to the observed concentrations by approximately an order of magnitude. The marine aerosol is not in steady state between the ocean emissions and dry deposition—cloud processing and wet deposition is necessary to balance the sources thereby simulating realistic concentrations. Despite this, several studies of the sea spray source, some of them deriving parametrizations, build on the assumption that the aerosol emissions are in steady state with the dry deposition (for example Fairall et al., 1983; Smith et al., 1993). This is not a method to be recommended in the submicrometre range. As noted in several experimental studies, for example Hoppel et al. (1986), cloud processing is essential also for the shape of the marine aerosol size distribution, especially for the formation of the so-called Hoppel-minimum which leads to a bimodal aerosol size distribution.

4.4. *Changes in activation diameter behind CNN trends*

The smallest size of activation varies between cloud cycles depending on the updraft velocity and the composition of the clusters in the critical size range as well as the kinetic limitations of droplet growth (e.g. Nenes et al., 2001). The latter means that the higher the accumulation mode concentration is, the lower the effective supersaturation rises and thus the larger the smallest size of activation is. Figure 12 shows how water temperature, DMS emissions and wind speed affect what sized particles are activated as cloud droplets. We see that although the smallest activation diameters are relatively stable, they increase with increasing temperature, DMS level and wind speed.

In Fig. 12a a gradual shift towards smaller activation sizes with decreasing sea water temperature is evident. As the number of particles larger than 200 nm D_p decreases with decreasing temperature (Fig. 4), the cloud activation scheme produces larger supersaturations, which enable smaller particles to be activated as cloud drops. This is not in contradiction with our earlier conclusion that the CDNC increases with increasing water temperature (Fig. 5b), because this effect is caused by the increase in the number of particles larger than 200 nm D_p with increasing temperature. Figure 12a also explains why the decrease in sizes $D_p < 40$ nm with increasing temperature can be seen in aerosol concentration (Fig. 5a), but not in the CDNC (Fig. 5b): this is because the very smallest sizes are hardly ever activated, especially when the sea water is warm.

Similar reasoning can also explain the absence of a clear trend in the CDNC with increasing DMS water concentration (and emissions). Despite the fact that one can see an increase in number concentration for particle with $D_p > 100$ nm with increasing DMS emissions in Fig. 6, this is a shift in size, not a real production of new particles. As more and more particles with $D_p > 100$ nm are available as cloud droplets, the cloud scheme distributes the water on these particles producing lower supersaturation, so that less of the particles with $D_p < 100$ nm are activated (see Fig. 12b). These results in only a weak CDNC net trend (see Fig. 7b). It must be remembered, however, that we do not simulate here the effect of changes in DMS on secondary particle formation in the FT.

The strong increase in particles at all diameters with increasing wind speed, as seen in Fig. 10, provides a large concentration of particles above 100 nm diameter that can act as cloud droplets, lowering the supersaturation so that less and less of the particles

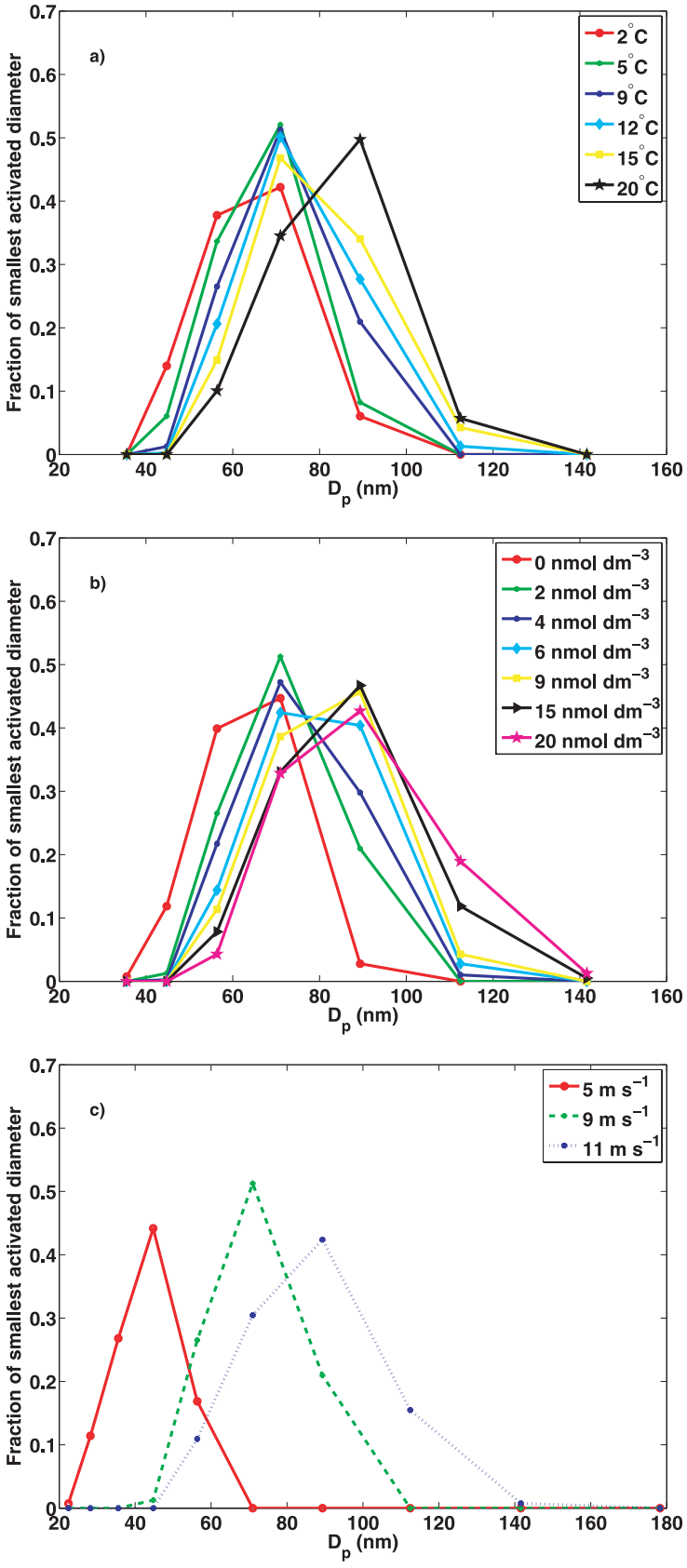

Fig. 12. Frequency distributions of the smallest activated particle size for individual 11-d simulation cycles using the Köhler equation. (a) For different water temperatures when DMS is 1.8 nmol dm^{-3} and wind speed is 9 m s^{-1}. (b) For different DMS concentrations in the water when wind speed is 9 m s^{-1} and water temperature is 9 °C. (c) For different wind speeds when water temperature is 9 °C and DMS concentration 1.8 nmol dm^{-3}.

below 100 nm diameter are activated. This shifts the most frequent minimum diameter that is activated to smaller sizes (Fig. 12c) as the wind speed decreases. However, unlike in the case of increasing DMS, this is not enough to compensate for the decreased aerosol number concentration. As a result of this, we observe a strong relationship between the aerosol number and CDNC and wind speed, as seen in Fig. 11.

4.5. Mass fraction

Several studies of aerosol mass sampled by impactors and chemical analysis in remote marine atmospheres show that sea salt dominates the mass in both the submicrometre and supermicrometre diameter range (e.g. Quinn et al., 2000; Cavalli et al., 2004; Quinn and Bates, 2005), which is in agreement with our results (Table 2). Andreae et al. (1999) has shown that the mass of sulphate in the supermicrometre range can be larger than the mass of sulphate in the submicrometre range. Traditional chemical analysis of the aerosol mass size distribution is limited to sizes larger than ~50 nm D_p, but other methods offer some information even about particles smaller than this. For example Swietlicki et al. (2000) shows that the hygroscopicity of marine aerosol particles below 100 nm diameter is often not as high as would be expected if the aerosols were made of sea-salt. Instead the observed hygroscopic growth rates resemble more ammonium sulphate or organic compounds. Such measurements have been used as an evidence for the absence of high hygroscopicity aerosols in the submicrometre range, and especially below 100 nm. However, Nilsson et al. (2001) showed that hygroscopic tandem differential mobility analyser (H-TDMA) measurements are not necessarily able to catch the freshly emitted sea spray aerosols even when such are shown by direct in situ eddy covariance flux measurements. This is probably because of the large concentration of aged sea spray aerosols that can be coated by secondary condensed material.

This can be seen also in Fig. 13a, which shows that our results are consistent with low hygroscopicity of submicrometre and sub-100 nm diameter marine particles. The model indicates that the aerosol is dominated by aged aerosols, in practise always, except perhaps directly after a heavy rain. Below 400 nm diameter, on average at least 20% of the mass is sulphate, which is enough to cover the original sea salt particle surface. In the Aitken and accumulation mode particles 30 and 70% of the average mass, respectively, sometimes even more, is sulphate. This is understandable as these modes themselves do not form from the sea spray but are formed from DMS derived sulphate on the original sea salt aerosols (Fig. 6). All in all, this explains the good agreement between our model results and the observed sea salt and sulphate masses (see Table 2). Figure 13a also shows that additional DMS emissions increase the sulphate fraction and shift its modal maximum in the Aitken and accumulation modes to larger sizes. Entrainment on the other hand increases the amount of sulphate in the Aitken mode and removes the local sea salt mass maximum between the Aitken and accumulation modes, see Fig. 9.

An increasing wind speed does not only increase the number concentration throughout the size distribution in agreement with Fig. 1b, but it also changes the fractioning between sea salt and sulphate, see Fig. 13b. When the wind speed increases the fraction of sea salt decreases in the Aitken mode and increases in accumulation mode particles. For D_p 300 nm the sea salt fraction increases from 30 to 80% when the wind speed increase from 5 to 11 ms^{-1}. Between 5 and 9 ms^{-1} the Aitken mode sulphate can be seen to migrate to larger sizes as a sign of more sulphate available at higher wind speed, but then the Aitken mode sulphate appears to stay at the same size, which is an indirect effect of the removal of larger particles by cloud droplet activation. In even larger sizes we simply see the gradual shift in sulphate maxima caused by the relative change in source strength when sea salt production change differently than DMS emissions

5. Summary and conclusions

This study has investigated the different processes affecting the marine aerosol size distribution. The key findings of the study are summarized below:

1. The combination of a primary sea salt source, secondary sulphate, and cloud processing form a bimodal size distribution characteristic for the marine aerosol. Sea-salt forms a spine for the size distribution, although in an aged distribution sulphate constitutes 20–80% of the Aitken and accumulation mode masses.

2. Accounting for all the relevant source, loss and aging mechanisms in the marine boundary layer, we are able to reproduce the sea-salt size distributions derived by the concentration parametrization by O'Dowd et al. (1997) using the Mårtensson et al. (2003) emission parametrization in an aerosol microphysics model and measured environmental conditions of O'Dowd et al. However, the shape of the size distribution, but not so much the aerosol number, is strongly dependent on environmental parameters, such as water temperature and DMS emissions. This implies that O'Dowd et al. (1997) cannot be generalized to other waters, seasons and weather conditions.

3. It is obvious that the marine aerosol cannot be in equilibrium without cloud processes and precipitation. This has implications among other things for those emission estimates in literature that are based on equilibrium balance between emissions and dry deposition.

4. DMS emissions change the mass concentration of marine aerosol and leads to the formation of Aitken and accumulation modes on the original sea salt aerosol. When both modes are validated with the size distribution from Heintzenberg et al. (2004), the simulated Atiken mode in particular shows a high probability of being found in a pristine marine atmosphere. When

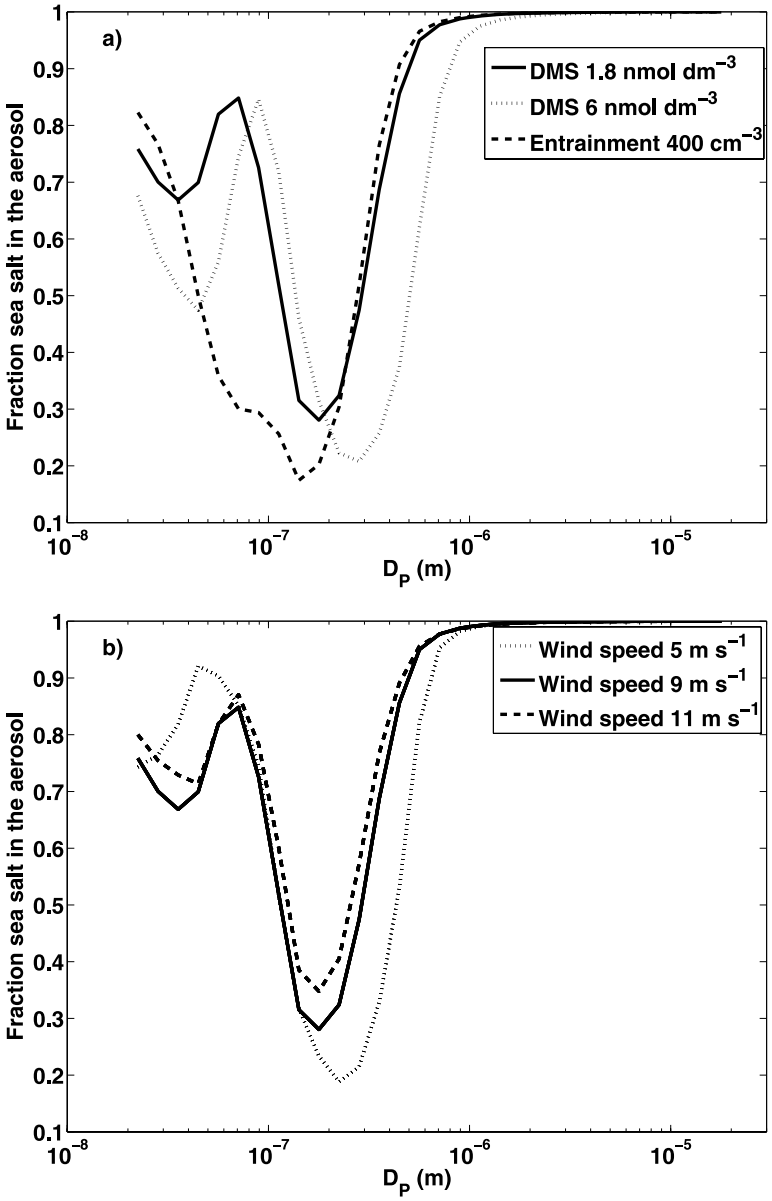

Fig. 13. (a) The fraction of sea salt mass in the aerosols; solid curve is for the base case when DMS in the water is 1.8 nmol dm^{-3}, dotted curve when the DMS in the water is 6 nmol dm^{-3} and dashed curve includes entrainment from the free troposphere with an aerosol concentration of 400 particles cm^{-3} (DMS in the water is 1.8 nmol dm^{-3}). (b) The fraction of sea salt mass in the aerosols for different wind speed; solid curve is for the base case when the wind speed is 9 ms^{-1}, dashed curve shows the mean sea salt fraction when the wind speed is 11 ms^{-1} and the dotted curve when wind speed is 5 ms^{-1}.

entrainment from FT is negligible, DMS also creates a maximum in the total number at rather small emissions, while not having a net effect on the CDNC. Particle entrainment from the FT has a strong effect on the marine boundary layer particle number and CDNC.

5. The effect of sea water temperature produces a maximum in number concentration for temperate waters, and a minimum for tropical waters. The CDNC on the other hand has a gradual but modest increase with increasing temperature.

6. Increasing wind speed increases the CDNC less than it increases the total aerosol number, since cloud activation of large particles at high wind speeds consumes so much water vapour that the minimum activation diameter increases. Despite this the CDNC is a strong power function of the wind speed, although the dependence is weaker than in the source parametrization. We find wind speed to be the dominant factor determining the CDNC in the absence of entrainment from FT.

In these first sensitivity tests only one parameter at a time has been changed from the base case, however one can expect some of the input parameters to be correlated both spatially and temporally. For example, subtropical locations generally will have less wind and fewer clouds than mid-high latitude locations. Also one can expect higher wind during cloudy periods in mid-high latitude locations. How these possible interactions change the size distribution will be investigated in future simulations. There is also a chance that the effects of different parameters cancel each other leaving the size distribution unchanged, but a

full exploration of the parameter space of the system is outside of the scope of these initial tests.

One important source of aerosol mass in biological productive areas, which should be included in the future studies, is organic matter from the ocean, but no parametrization is yet available for its source emission. Further research is required also to study the effect of complex cloud processes (here we use only low stratus clouds with fixed height) and varying boundary layer height, although large effects of different dynamic processes, clouds and precipitation are shown also with our simplified approach. In the future we will make use of 3-D trajectories to prescribe the transport over the ocean and the environmental parameters such as wind speed, temperature, boundary layer depth, cloudiness and precipitation This will allow us to make Lagrangian model simulations of the marine aerosol where we allow the different competing aerosol sources, sinks and transformation process to form an aerosol that can be compared with observed aerosols.

Acknowledgments

We would like to thank the Nordic Centre of Excellence for Biosphere Aerosol Cloud Climate Interaction (BACCI), the Swedish Research Council (VR), the Finnish Academy, the UK Natural Environment Research Council (NERC) and the European Commission on the projects QUEST (Quantification of aerosol formation in the European boundary layer) and MAP (Marine Aerosol Production from Natural Sources).

References

Andreae, M. O., Talbot, R. W., Berresheim, H. and Beecher K. M. 1990. Precipitation chemistry in central amazonia. *J. Geophys. Res.* **95**(D10), 16987–16999.

Andreae, M. O., Elbert, W., Cai, Y., Andreae, T. W. and Gras, J. 1999. Non-sea-salt sulfate, methanesulfonate, and nitrate aerosol concentrations and size distributions at Cape Grim, Tasmania. *J. Geophys. Res.-Atmos.* **104**, 21695–21706.

Aranami, K., Watanabe, S., Tsunogai, S., Ohki, A., Miura, K. and co-authors. 2002. Chemical assessment of oceanic and terrestrial sulfur in the marine boundary layer over the northern North Pacific during summer. *J. Atmos. Chem.* **41**, 49–66.

Barahona, D., West, R. E. L., Stier, P., Romakkaniemi, S., Kokkola, H., and co-authors. 2010. Comprehensively accounting for the effect of giant CCN in cloud activation parameterizations. *Atmos. Chem. Phys.*, **10**, 2467–2473, www.atmos-chem-phys.net/10/2467/2010/.

Bates, T. S., Quinn, P. K., Covert, D. S., Coffman, D. J., Johnson, J. E. and co-authors. 2000. Aerosol physical properties and processes in the lower marine boundary layer: a comparison of shipboard sub-micron data from ACE-1 and ACE-2. *Tellus* **52B**, 258–272.

Bates, T. S., Coffman, D., Covert, D. S. and Quinn, P. 2002. Regional marine boundary layer aerosol size distributions in the Indian, Atlantic, and Pacific Oceans: a comparison of INDOEX measurements with ACE-1, ACE-2, and Aerosols99. *J. Geophys. Res.*, **107**(D19), 8026, doi:10.1029/2001JD001174.

Berresheim, H., Elste, T., Tremmel, H. G., Allen, A. G., Hansson, H. C. and co-authors. 2002. Gas-aerosol relationships of H2SO4, MSA, and OH: observations in the coastal marine boundary layer at Mace Head, Ireland. *J. Geophys. Res.*, **107**(D19), 8100, doi:10.1029/2000JD000229.

Capaldo, K. P., Kasibhatla, P. and Pandis, S. N. 1999. Is aerosol production within the remote marine boundary layer sufficient to maintain observed concentrations? *J. Geophys. Res.* **104**, 3483–3500.

Cavalli, F., Facchini, M. C., Decesari, S., Mircea, M., Emblico, L. and co-authors. 2004. Advances in characterization of size-resolved organic matter in marine aerosol over the North Atlantic. *J. Geophys. Res* **109**, D24215, doi:10.1029/2004JD005137.

Charlson, R. J., Lovelock, J. E., Andreae, M. O. and Warren, S. G.: 1987. Oceanic phytoplankton, atmospheric sulphur, cloud albedo and climate. *Nature* **326**, 655–661.

Chuang, P. Y., Collins, D. R., Pawlowska, H., Snider, J. R., Jonsson, H. H. and co-authors. 2000. CCN measurements during ACE-2 and their relationship to cloud microphysical properties. *Tellus* **52**B, 843–867.

Clarke, A. D. and Kapustin, V. 2002. A pacific aerosol survey. Part I: a decade of data on particle production, transport, evolution, and mixing in the troposphere. *J. Atmos. Sc.* **59**, 363–382.

Clarke, A. D., Li, Z. and Litchy, M. 1996. Aerosol dynamics in the equatorial Pacific Marine boundary layer: microphysics, diurnal cycles and entrainment. *Geophys. Res. Lett.* **23**(7), 733–736.

Clarke, A. D., Davis D., Kapustin, V. N., Eisele, F., Chen, G. and co-authors. 1998. Particle nucleation in the tropical boundary layer and its coupling to marine sulfur sources. *Science* **282**, 89–92, doi:10.1126/science.282.5386.89.

Clarke, A. D., Owens, S. R. and Zhou, J. 2006. An ultrafine sea-salt flux from breaking waves: implications for cloud condensation nuclei in the remote marine atmosphere. *J. Geophys Res.*, **111**, D06202, doi:10.1029/2005JD006565.

Covert, D., Gras, J., Wiedensohler, A. and Stratmann, F. 1998. Comparison of directly measured CCN with CCN modeled from the number-size distribution in the marine boundary layer during ACE 1 at Cape Grim, Tasmania. *J. Geophys. Res.-Atmos.* **103**, 16597–16608.

Fairall, C. W., Davidson, K. L. and Schacher, G. E. 1983. An analysis of the surface production of sea-salt aerosol. *Tellus* **35B**, 31–39.

Geever, M., O'Dowd, C. D., van Ekeren, S., Flanagan, R., Nilsson, E. D. and co-authors. 2005. Sub-micron sea-spray fluxes. *Geophys. Res. Lett.* **32**, L15810, doi:10.1029/2005GL023081.

Grini, A., Korhonen, H., Lehtinen, K. E. J., Isaksen, I. S. A. and Kulmala, M. 2005. A combined photochemistry/aerosol dynamics model: model development and a study of new particle formation. *Boreal Environ. Res.* **10**, 525–541.

Heintzenberg, J, Covert, D. C. and Van Dingenen, R. 2000. Size distribution and chemical composition of marine aerosols: a compilation and review. *Tellus* **52B**(4), 1104–1122.

Heintzenberg, J., Birmili, W., Wiedensohler, A., Nowak, A. and Tuch, T. 2004. Structure, variability and persistence of the submicrometre marine aerosol. *Tellus* **56B**, 357–367.

Hoppel, W. A. and Frick, G. M. 1990. Submicron aerosol size distributions measured over the tropical and south pacific. *Atmos. Environ.* **24**, 645–659.

Hoppel W. A., Frick, G. M. and Larson, R. E. 1986. Effect of nonprecipitating clouds on the aerosol size distribution in the marine boundary layer. *Geophys. Res. Lett.* **13**(2), 125–128.

Hoppel, W. A., Fitzgerald, J. W., Frick, G. M. and Larson, R. E. 1990. Aerosol size distributions and optical properties found in the marine boundary layer over the Atlantic Ocean. *J. Geophys. Res.* **95**, 3659–3686.

Huebert, B., Bates, T., Russell, P., Shi, G., Kim, Y. and co-authors. 2003. An overview of ACE Asia: strategies for quantifying the relationships between Asian aerosols and their climatic impacts. *J. Geophys. Res.-Atmos.* **108**(D23), 8633, doi:10.1029/2003JD003550.

IPCC. 2001. Climate ChanInge 2001: the Scientific Basis. In: *Contribution of Working Group I to the Third Assessment Report of the Intergovernmental Panel on Climate Change* (eds Houghton, J. T., Y. Ding, D. J. Griggs, M. Noguer, P. J. van der Linden, X. Dai, K.Maskell, and C. A. Johnson). Cambridge University Press, Cambridge, United Kingdom and New York, NY, USA, 881pp.

Laakso, L., Grönholm, T., Rannik, Ü., Vehkamäki, H., Kosmale, M., and co-authors. 2003. Ultrafine particle scavenging coefficients calculated from six years field measurements. *Atmos. Environ.* **37**, 3605–3613.

Kloster, S., Feichter, J., Reimer, E. M., Six, K. D., Stier, P. and co-authors. 2006. DMS cycle in the marine ocean-atmosphere system – a global model study. *Biogeosciences* **3**, 29–51.

Komppula, M., Sihto, S. L., Korhonen, H., Lihavainen, H., Kerminen, V. M. and co-authors. 2006. New particle formation in air mass transported between two measurement sites in Northern Finland. *Atmos. Chem Phys* **6**, 2811–2824.

Korhonen, H., Lehtinen, K. E. J. and Kulmala, M. 2004. Aeroeol dynamic model UHMA: model development and validitation. *Atmos. Chem Phys.*, 757–771, Sref-ID: 1680–7324/acp/2004–4-757.

Korhonen, H., Carslaw, K. S., Spracklen, D. V., Mann, G. W. and Woodhouse, M. T. 2008. Influence of oceanic dimethyl sulfide emissions on cloud condensation nuclei concentrations and seasonality over the remote Southern Hemisphere oceans: a global model study. *J. Geophys. Res.* **113**, D15204, doi:10.1029/2007JD009718.

Leck, C. and Bigg, E. K. 2005a. Source and evolution of the marine aerosol—a new perspective. *Geophys. Res. Lett.*, **32**, L19803, doi:10.1029/2005GL023651.

Leck, C. and Bigg, E. K. 2005b. Biogenic particles in the surface microlayer and overlaying atmosphere in the central Arctic Ocean during summer. *Tellus, Ser. A and Ser. B*, **57B**, 305–316.

Mårtensson, E. M., Nilsson, E. D., de Leeuw, G., Cohen, L. H. and Hansson, H. C. 2003. Laboratory simulations and parameterization of the primary marine aerosol production. *J. Geophys. Res.* **108**, 4297, doi:10.1029/2002JD002263.

Middlebrook, A. M., Murphy, D. M. and Thomson, D. S. 1998. Observations of organic material in individual marine particles at Cape Grim during the First Aerosol Characterisation Experiment (ACE 1). *J. Geophys. Res.* **103**, 16475–16483.

Monahan, E. C. and O'Muircheartaigh, I. 1980. Optimal power-law description of oceanic whitecap coverage dependence on wind speed. *J. Phys. Oceanogr.* **10**, 2094–2099.

Monahan, E. C., Spiel D. E. and Davidson, K. L. 1986. A model of marine aerosol generation via whitecaps and wave disruption. In: *Oceanic Whitecaps* (eds E. C. Monahan, and G. MacNiochaill). D. Reidel Publ. Comp., Norwell, MA, 167–193.

Murphy, D. M., Anderson, J. R., Quinn, P. K., McInnes, L. M., Brechtelk, F. J. and co-authors. 1998. Influence of sea-salt on aerosol radiative propertiesin the Southern Ocean marine boundary layer. *Nature* **392**, 62– 65.

Nenes, A., Ghan, S., Abdul-Razzak, H., Chuang, P. Y. and Seinfeld, J. H. 2001. Kinetic limitations on cloud droplet formation and impact on cloud albedo. *Tellus* **53B**, 133–149.

Nightingale, P., Malin, G., Law, C., Watson, A., Liss, P. and co-authors. 2000. In situ evaluation of air-sea exchange parameterizations using novel conservative and volatile tracers. *Glob. Biogeochem. Cycles* **14**, 373–387.

Nilsson, E. D., Rannik, Ü., Swietlicki, E., Leck, C., Aalto, P. P. and co-authors. 2001. Turbulent aerosol fluxes over the Arctic Ocean 2. Wind-driven sources from the sea. *J. Geophys. Res*. **106**, 32111–32124.

Nilsson, E. D., Mårtensson, E. M., Van Ekeren, J. S., de Leeuw, G., Moerman, M., and co-authors. 2007. Primary marine aerosol emissions: size resolved eddy covariance measurements with estimates of sea salt and organic carbon fractions. *Atmos. Chem. Phys. Discuss* **7**, 13345–13400.

Norris, S. J., Brooks, I. M., de Leeuw, G., Smith, M. H., Moerman, M. and co-authors. 2008. Eddy covariance measurements of sea spray particles over the Atlantic Ocean. *Atmos. Chem. Phys.* **8**, 555–563.

O'Dowd, C. D. and Smith, M. H. 1993. Physiochemical properties of aerosols over the Northeast Atlantic: evidence for wind-related submicron sea-salt aerosol production. *J. Geophys. Res.* **98**, 1137–1149.

O'Dowd, C. D., Smith, M. H., Consterdine, I. E. and Lowe, J. A. 1997. Marine aerosol, sea-salt, and the marine sulphur cycle: a short review. *Atmos. Environ* **31**, 73–80.

Pham, M., Muller, J. F., Brasseur, G., Granier, C. and Mégie, G. 1995. A three-dimensional study of the tropospheric sulfur cycle. *J. Geophys. Res.* **100**, 26061–26092.

Pierce, J. R. and Adams, P. J. 2006. Global evaluation of CCN formation by direct emission of sea salt and growth of ultrafine sea salt. *J. Geophys. Res.* **111**, D06203, doi:10.1029/2005JD006186.

Quinn, P. K. and Bates, T. S. 2005. Regional aerosol properties: comparisons of boundary layer measurements from ACE 1, ACE 2, Aerosols99, INDOEX, ACE Asia, TARFOX, and NEAQS. *J. Geophys. Res.* **110**, D14202, doi:10.1029/2004JD004755.

Quinn, P. K. and Coffman, D. J. 1999. Comment on "Contribution of different aerosol species to the global aerosol extinction optical thickness: estimates from model results" by Tegen et al. *J. Geophys. Res.-Atmos.* **104**, 4241–4248.

Quinn, P. K., Bates, T. S., Coffman, D. J., Miller, T. L., Johnson, J. E. and co-authors. 2000. A comparison of aerosol chemical and optical properties from the 1st and 2nd Aerosol Characterization Experiments. *Tellus* **52B**, 239–257.

Raes, F. 1995. Entrainment of free tropospheric aerosols as a regulating mechanism for cloud condensation nuclei in the remote marine boundary layer. *J. Geophys. Res*, **100**(D2): 2893–2903.

Russell, L. M., Hawkins, L. N., Frossard, A. A., Quinn, P. K. and Bates, T. S. 2010. Carbohydrate-like composition of submicron atmospheric particles and their production from ocean bubble bursting. www.pnas.org/cgi/doi/10.1073/pnas.0908905107

Russell, P. and Heintzenberg, J. 2000. An overview of the ACE 2 Clear Sky Column Closure experiment (CLEARCOLUMN). *Tellus* **52B**, 463–483.

Seinfeld, J. H. and Pandis, S. N. 1998. *Atmospheric Chemistry and Physics: From Air Pollution to Climate Change*. John Wiley & Sons, Inc., NY.

Slinn, S. A. and Slinn, W. G. N. 1980. Predictions for particle deposition on natural waters. *Atmos. Environ*, **14**, 1013–1016.

Smith, M. H., Park, P. M. and Consterdine, I. E. 1993. Marine aerosol concentrations and estimated fluxes over the ocean. *Q. J. R. Meteorol. Soc*. **119**, 809– 824.

Spracklen, D. V., Pringle, K. J., Carslaw, K. S., Mann, G. W., Manktelow, P. and co-authors. 2007. Evaluation of a global aerosol microphysics model against size-resolved particle statistics in the marine atmosphere. *Atmos. Chem. Phys.* **7**, 2073–2090.

Swietlicki, E., Zhou, J., Covert, D. S., Hameri, K., Busch, B. and co-authors. 2000. Hygroscopic properties of aerosolparticles in the north-eastern Atlantic during ACE-2. *Tellus* **52B**, 201–227.

Talbot, R. W., Andreae, M. O., Berresheim, H., Artaxo, P., Garstang, M. and co-authors. 1990. Aerosol chemistry during the wet season in central amazonia: the influence of long-range transport. *J. Geophys. Res.* **95**(D10), 16,955–16,969.

Tunved, P., Korhonen, H., Ström, J., Hansson, H-C., Lehtinen, K. E. J. and co-authors. 2006. Is nucleation capable of explaining observed aerosol number increase during southerly transport over Scandinavia? *Tellus* **58B**, 129–140.

Warren, S. G., Hahn, C. J., Eastman, R. and Rigor I. G. 2006. Climatic atlas of clouds over land and ocean. http://www.atmos.washington.edu/CloudMap.

Weber, R. J., Chen, G., Davis, D. D., Mauldin, R. L., Tanner, D. J. and co-authors. 2001. Measurements of enhanced H2SO4 and 3–4 nm particles near a frontal cloud during the First Aerosol Characterization Experiment (ACE 1). *J. Geophys. Res.-Atmos*. **106**, 24107–24117.

Wiedensohler, A., Covert, D. S., Swietlicki, E., Aalto, P., Heintzenberg, J. and co-authors. 1996. Occurrence of an ultrafine particle mode less than 20 nm in diameter in the marine boundary layer during Arctic summer and autumn. *Tellus* **48B**, 213–222.

Yoon Y. J. and Brimblecombe, P. 2002. Modelling the contribution of sea-salt and dimethyl sulphide derived aerosol to marine CCN. *Atmos. Chem. and Phys.* **2**, 17–30.